

Gazi Üniversitesi **Fen Bilimleri Dergisi**PART C: TASARIM VE TEKNOLOJİ

Gazi University Journal of Science PART C: DESIGN AND

TECHNOLOGY



GU J Sci, Part C, 13(3): 1240-1252 (2025)

Determination of Radiation Shielding Properties of Magnesium Oxychloride Cement with Acidic and Basic Pumice Aggregate

Şemsettin KILINÇARSLAN¹ D, Yasemin ŞİMŞEK TÜRKER^{1*}D, Nuri IŞILDAR²D

¹Süleyman Demirel University, Faculty of Engineering and Natural Sciences, Department of Engineering, Isparta, Turkey

Article Info

Research article Received: 01/05/2025 Revision: 09/09/2025 Accepted: 12/09/2025

Keywords

Magnesium oxychloride Cement Pumice Radiation shielding **Makale Bilgisi**

Araştırma makalesi Başvuru: 01/05/2025 Düzeltme: 09/09/2025 Kabul: 12/09/2025

Anahtar Kelimeler

Magnezyum oksiklorür Çimento Pomza Radyasyon zırhlama

Graphical/Tabular Abstract (Grafik Özet)

This study investigates the radiation shielding properties of magnesium oxychloride cement (MOC) using acidic and basic pumice aggregates. Experimental tests and XCOM simulations revealed that acidic pumice provided superior attenuation, especially at low energies, while basic pumice offered advantages in mass efficiency. Findings highlight potential of MOC as an eco-friendly, functional construction material.

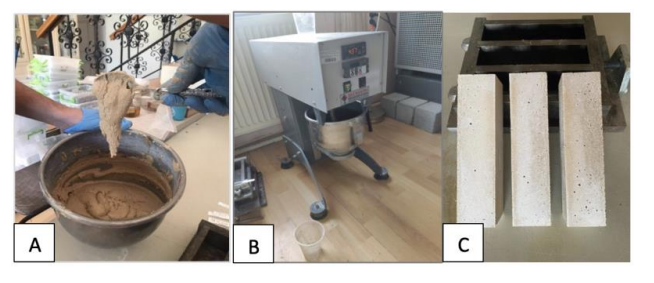


Figure 2. Preparation of samples A: Pouring ingredients into a container, B: Mixing the ingredients, C: Removing the samples from the mold/Şekil 2: Numunelerin hazırlanması A: Malzemelerin bir kaba boşaltılması, B: Malzemelerin karıştırılması, C: Numunelerin kalıptan çıkarılması

Highlights (Önemli noktalar)

- Acidic pumice aggregate showed superior radiation shielding, especially at low energies.
 / Asidik pomza agregası düşük enerjilerde üstün radyasyon zırhlama özelliği göstermiştir.
- Basic pumice provided better mass attenuation efficiency, particularly at higher energies.
 / Bazik pomza özellikle yüksek enerjilerde daha iyi kütle zayıflatma verimliliği sağlamıştır.
- Experimental results were slightly higher than XCOM predictions, confirming material effectiveness. / Deneysel sonuçlar XCOM tahminlerinden biraz daha yüksek çıkmış, malzemenin etkinliğini doğrulamıştır.
- Findings highlight the potential of MOC-based concretes as eco-friendly functional building materials. / Bulgular, MOC esaslı betonların çevre dostu işlevsel yapı malzemeleri olma potansiyelini ortaya koymaktadır.

Aim (Amaç): This study aims to investigate the radiation shielding properties of magnesium oxychloride cement concretes containing acidic and basic pumice aggregates. / Bu çalışma, asidik ve bazik pomza agregaları içeren magnezyum oksiklorür çimentosu betonlarının radyasyon zırhlama özelliklerini incelemeyi amaçlamaktadır.

Originality (Özgünlük): The study presents a comparative evaluation of acidic and basic pumice in MOC concretes, providing new insights into their effectiveness in radiation shielding applications. /Çalışma, MOC betonlarında asidik ve bazik pomzanın karşılaştırmalı değerlendirmesini sunarak radyasyon zırhlama uygulamalarındaki etkinliklerine dair yeni bulgular ortaya koymaktadır.

Results (Bulgular): Experimental findings showed that acidic pumice concretes have higher attenuation capacity at lower energies, while basic pumice concretes offer mass efficiency advantages at higher energies. /Deneysel bulgular, asidik pomza betonlarının düşük enerjilerde daha yüksek zayıflatma kapasitesine sahip olduğunu, bazik pomza betonlarının ise yüksek enerjilerde kütle verimliliği avantajı sunduğunu göstermiştir.

Conclusion (Sonuç): Acidic pumice is more effective for compact shielding applications, while basic pumice is suitable for lightweight structures, highlighting the versatility of MOC-based concretes. /Asidik pomza kompakt zırhlama uygulamaları için daha etkili, bazik pomza ise hafif yapılar için uygun bulunmuş, bu durum MOC esaslı betonların çok yönlülüğünü ortaya koymuştur.

²Süleyman Demirel University, Natural and Industrial Building Material Applied Center, Isparta, Türkiye



Gazi Üniversitesi **Fen Bilimleri Dergisi** PART C: TASARIM VE TEKNOLOJİ

Gazi University

Journal of Science

PART C: DESIGN AND

TECHNOLOGY



A BHILLIAM TO A BANK TO

http://dergipark.gov.tr/gujsc

Determination of Radiation Shielding Properties of Magnesium Oxychloride Cement with Acidic and Basic Pumice Aggregate

Şemsettin KILINÇARSLAN¹, Yasemin ŞİMŞEK TÜRKER^{1*}, Nuri IŞILDAR²

Article Info

Research article Received: 01/05/2025 Revision: 09/09/2025 Accepted: 12/09/2025

Keywords

Magnesium oxychloride Cement Pumice Radiation shielding

Abstract

New-generation cements are increasingly being investigated due to their potential for low carbon emissions and reduced environmental impacts. Magnesium oxychloride cement (MOC) is an innovative binder formed by the reaction of magnesia powder with MgCl₂ solution, offering properties such as high early strength, good workability, low density, and fire resistance. In this study, pumice was used as an aggregate in MOC-based concrete, and the radiation shielding properties of the resulting concrete were investigated using both experimental methods and XCOM calculations. Basic and acidic pumice aggregates, commonly used in lightweight concrete production, were compared. The results showed that experimental radiation shielding values were slightly higher than XCOM predictions, particularly at low energies. This highlights the critical importance of material selection and the potential for innovative mix designs to enhance concrete performance.

Asidik ve Bazik Pomza Agregalı Magnezyum Oksiklorür Çimentosunun Radyasyon Zırhlama Özelliklerinin Belirlenmesi

Makale Bilgisi

Araştırma makalesi Başvuru: 01/05/2025 Düzeltme: 09/09/2025 Kabul: 12/09/2025

Anahtar Kelimeler

Magnezyum oksiklorür Çimento Pomza Radyasyon zırhlama Yeni nesil çimentolar, düşük karbon emisyonları ve çevresel etkileri azaltma potansiyelleri nedeniyle giderek daha fazla araştırılmaktadır. Magnezyum oksiklorür çimentosu (MOC), magnezya tozunun MgCl² çözeltisi ile reaksiyonu sonucu oluşan, yüksek erken dayanım, iyi işlenebilirlik, düşük yoğunluk ve yangına dayanıklılık gibi özelliklere sahip yenilikçi bir bağlayıcıdır. Bu çalışmada, MOC esaslı betonda agrega olarak pomza kullanılmış ve elde edilen betonun radyasyon zırhlama özellikleri hem deneysel yöntemlerle hem de XCOM hesaplamalarıyla incelenmiştir. Hafif beton üretiminde yaygın olarak tercih edilen bazik ve asidik pomza agregaları karşılaştırılmıştır. Sonuçlar, deneysel radyasyon tutuculuk değerlerinin özellikle düşük enerjilerde XCOM tahminlerinden biraz daha yüksek olduğunu göstermiştir. Bu durum, malzeme seçiminin kritik önemini ve betonun performansını artırmak için yenilikçi karışım tasarımlarının potansiyelini ortaya koymaktadır.

1. INTRODUCTION (GİRİŞ)

Magnesium-based cement, also known as Sorel cement, differs from Portland cement in terms of production technology and is a new-generation binder that is being researched to prevent Portland cement from releasing high carbon and damaging the environment structure. Magnesium-based cement is a combination of a cross-linking agent that reacts with the calcined magnesite component to form a solidified binder matrix. Concrete mixtures prepared with magnesium oxychloride cement (MOC) can have high compressive strength between 55 and 69 MPa within 48 hours when properly formulated. Concrete produced with MOC is a very stable building material against heating,

freezing, and thawing cycles. MOC is produced by mixing water, magnesium oxide (MgO), and magnesium chloride (MgCl2) for a certain period [1,2]. MOC has a shorter setting time than regular Portland cement, but it has less water resistance. A certain amount of phosphoric acid is added to the mixture to minimize the disadvantage of MOC against water. The properties of MOC have been investigated in terms of MgO/MgCl₂ and molar ratios. The H₂O/MgCl₂ changes in MgO/MgCl₂ and H₂O/MgCl₂ molar ratios greatly affect the mechanical properties of MOC. The most preferred ranges for design purposes are 11-17 MgO/MgCl₂ and 12-18 H₂O/MgCl₂ for a binder with a majority of 5MgO MgCl₂·8H₂O (phase 5) crystals. However, the MgO/MgCl₂ mole ratio plays

¹Süleyman Demirel University, Faculty of Engineering and Natural Sciences, Department of Engineering, Isparta, Turkey

²Süleyman Demirel University, Natural and Industrial Building Material Applied Center, Isparta, Türkiye

a major role in determining the H₂O/MgCl₂ mole ratio, primarily to regulate the workability of the paste [3,4].

Research was conducted on various usage ratios of several MOC types, including 13 mol fixed magnesite, 12 mol water, and 0.5 to 1.9 mol magnesium chloride. It was found that as the amount of magnesium chloride used in MOC increased, the compressive strength, initial and final setting times, and water solubility values of the samples also increased. The maximum compressive strength value was found in the 1.5 mol magnesium chloride samples used in MOC. According to X-ray diffraction analysis (XRD) studies, Phase 5, 5 Mg (OH)₂•MgCl₂·6H₂O, gradually increased, while hydrated magnesia, Mg (OH)₂, gradually decreased. According to experiments using a scanning electron microscope (SEM), phase 5 needle-shaped crystals are very good at strengthening the MOC matrix. Using the sample with the best strength among those made using MOC, a nanocomposite containing SiC nanoparticles was created. It was stated that this composite does not carry the risk of grain growth and does not require melting or burning for sintering. With the high concentration of needleshaped reinforcing crystals in Phase 5, the increase of magnesium chloride in the matrix, and the nanosized aggregate particles of SiC, the production of stronger nanocomposites can be realized [4-6].

Pumice is a light and porous natural stone of volcanic origin. Formed by releasing gases during the rapid cooling and solidification of lava, this stone draws attention with its low density, high heat, and sound insulation properties. Pumice is an environmentally friendly and recyclable material, and it is used as an insulation material, especially in the construction sector, in the production of lightweight concrete and mortar [7,8]. Turkey, with its rich pumice reserves, produces in provinces such as Nevşehir, İsparta, Kayseri, Van, Agrı, and Bitlis, meeting both domestic market needs and exporting to the world. Thanks to its lightness, pumice, which reduces the weight of buildings and provides energy savings, is an indispensable material for the construction sector and other industries with its natural structure and versatile use [9-11]. For this reason, pumice is widely used in many construction products.

Pumice is a porous rock type formed because of volcanic activity. Pumice has been used as aggregate in the production of lightweight concrete in many countries of the world. Satisfactory concrete, lighter than normal concrete with good insulating characteristics, with high absorption and shrinkage, can be manufactured using pumice [12]. The pores in pumice are usually unconnected spaces. For these reasons, it is quite light, has low permeability, and has high heat and sound insulation [13, 14]. Pumice is widely used in many industries, especially in the construction sector. There are varieties of pumice, such as acidic pumice and basic pumice. Acidic pumice is rich in silica, usually containing 63% or more silica. It has more quartz and feldspar in terms of mineral composition. Basic pumice has a lower silica ratio, usually containing 45-52% silica [15-17]. Acidic pumice is light-colored, light gray, and cream colors, while Basic pumice is darker, dark gray, and black. Acidic pumice has a lower density because it is more porous, but Basic pumice is less porous and therefore has a higher density. Acidic pumice can contain a glassier structure, and the rapid cooling process limits crystallization. Basic Pumice Magma cools more slowly, so it can contain more crystalline mineral phases. These differences affect the physical and chemical properties of pumice and, therefore, its areas of use. Acidic and basic types of pumice are important examples to understand the diversity and versatile usability of this stone. The acidic and basic properties of pumice make it a versatile material for both industrial environmental applications. Both types of pumice are used in various areas to maintain sustainability and ecological balance [18-20].

The low pH level of acidic pumice allows it to be used effectively in applications with acidic properties. On the other hand, basic pumice stands out with its composition structure, which contains higher proportions of minerals such as iron and magnesium. This type of pumice can be used in applications that require alkaline properties, especially since it is stable in environments with basic pH levels. Its chemical composition is used in the definition of pumice. The chemical composition properties of acidic and basic pumice are given in Table 1, and the physical properties are given in Table 2 [21].

Table 1. Chemical properties of acidic and basic pumice samples (%) (Asidik ve bazik pomza örneklerinin kimyasal özellikleri (%))

Compound	Acidic Pumice	Basic Pumice
SiO_2	72.5	45.0
Al_2O_3	14.0	21.0
Fe_2O_3	2.5	7.0
CaO	0.9	11.0
MgO	0.6	7.0
Na ₂ O+K ₂ O	9.0	8.0
LOI	3.0	1
Compound	Acidic Pumice	Basic Pumice
SiO_2	72.5	45.0
Al_2O_3	14.0	21.0
Fe ₂ O ₃	2.5	7.0

Table 2. Physical properties of acidic and basic pumice samples (Asidik ve bazik pomza örneklerinin fiziksel özellikleri)

Properties	Acidic Pumice	Basic Pumice
Unit Volume Weight	613	1012
(kg/m^3)		
Water Absorption	20.8	9.6

2. MATERIALS AND METHODS (MATERYAL VE METOD)

In this study, MOC, Magnesium Oxide (MgO), and Magnesium Chloride (MgCl₂) prepared in certain proportions, were used as binders. The following chemicals were used for the syntheses: $MgCl_2 \cdot 6H_2O$ (>99%), MgO (>98%), and deionized water.

The ratio of 5 MgO to MgCl₂·6H₂O was used for the synthesis of a stoichiometric phase of MOC with a composition 5Mg(OH)₂·MgCl₂·8H₂O (termed as Phase 5, also known as Mg3(OH)₅Cl·4H₂O). To prepare the first sample, 30.6 g of MgCl₂·6H₂O was dissolved in 19.0 g of deionized water. In the next step, 30.4 g of magnesium oxide was added, and the of Phase 5:

$$5 MgO + MgCl_2 \cdot 6H_2O + 3 H_2O \cdot 5Mg(OH)_2 \cdot MgCl_2 \cdot 8H_2O$$
 (1)

Similarly, the stoichiometric Phase 3 $(3Mg(OH)_2 \cdot MgCl_2 \cdot 8H_2O)$ or $Mg_2(OH)_3Cl \cdot 4H_2O)$ was prepared by mixing MgO, MgCl₂·6H₂O and H₂O in the molar ratio 3:1:5. To prepare the second sample, 39.1 g of MgCl₂·6H₂O was dissolved in

17.3 g of deionized water. In the next step, 23.2 g of magnesium oxide was added, and the suspension was intensively stirred for 5 min. The formation of magnesium oxychloride cement MOC 3-1-8 is summarized in the following Equation (2):

$$3 MgO + MgCl_2 \cdot 6H_2O + 5 H_2O \rightarrow 3Mg(OH)_2 \cdot MgCl_2 \cdot 8H_2O.$$
 (2)

Suspensions were used to prepare samples. Isparta-Karakaya and Isparta-Gelincik pumice were used as aggregate. Sieve analysis was performed to standardize the granulometry of the aggregates used, and castings were made according to the determined granulometry. After the crushing process, one of the most important parameters to obtain high-strength concrete is sieve analysis. The dimensions of the aggregates should have a

distribution by the standards; that is, the general grain distribution should be known, or the aggregate grain distribution ratios should be adjusted correctly to provide a suitable composition and prevent grain segregation. In this study, acidic and basic pumice were used. First, MOC was produced with acidic pumice (MAP) and basic pumice (MBP). Isparta Karakaya and Isparta Gelincik Pumice are given in Figure 1.



Figure 1. Isparta Karakaya and Isparta Gelincik Pumice (Isparta Karakaya ve Isparta Gelincik Pomza)

The radiation shielding properties of the produced concrete samples were examined. Experiments were carried out on 3 samples from each series. The

production phase of the samples is given in Figure 2.

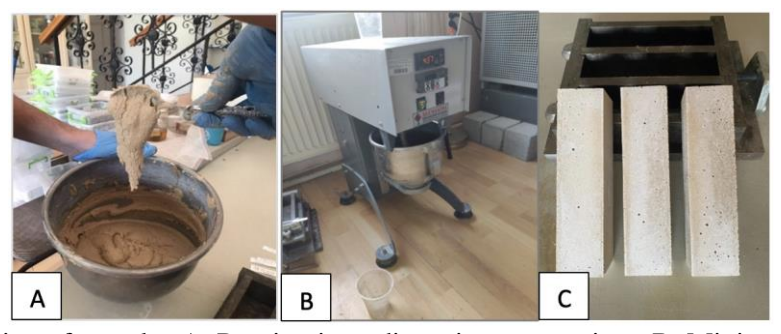


Figure 2. Preparation of samples A: Pouring ingredients into a container, B: Mixing the ingredients, C: Removing the samples from the mold (Numunelerin hazırlanması A: Malzemelerin bir kaba boşaltılması, B: Malzemelerin karıştırılması, C: Numunelerin kalıptan çıkarılması)

Experiments with radiation shielding were conducted in the Gamma Spectroscopy Laboratory. A gamma spectroscopy system uses the interaction of the emitted gamma rays with the NaI (TI) detector to distinguish them based on their energy. The radiation shielding experimental setup, Na (TI) scintillation detector, was used to evaluate radiation absorption coefficients. The scintillator, which is a sparkling substance, and the photomultiplier tube, which houses the photocathode, electrode, electron multipliers, and anode, are the two primary components of a scintillation detector. The gamma ray first enters the scintillator, where it interacts with certain solid, liquid, or gaseous materials known as scintillation phosphors to cause ionization and excitation. Gamma-ray-excited electrons return to their initial state and release light when the energy required to remove them from their environment is insufficient. Photomultiplier tubes gather the emitted light and transform it into a voltage pulse. The energy of the radiation determines the amplitude of this pulse. These detectors can also be used for energy separation and counting. With the aid of an amplifier, the gamma radiation-generated signals in the NaI (TI) detector are strengthened and shaped to offer the proper energy separation. The Multi-Channel Analyzer (MCC), which has 16384 channels, each of which represents an energy, receives the signal from the amplifier and transforms it into digital form. The analyzers digitally transformed data is shown as a spectrum on the screen. The high-voltage unit supplies power to the system [22, 23]. As seen in Figure 3, it will be ensured that the sample is equally spaced from the source and the detector during the trials.

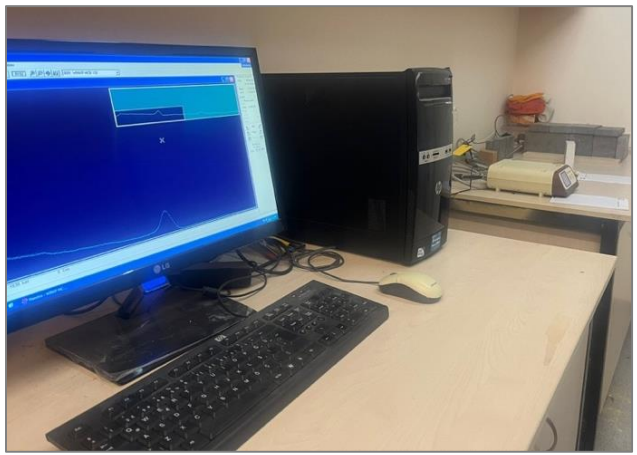


Figure 3. Schematic and real images of the detector and electronic devices that make up the gamma spectroscopy system (Gama spektroskopisi sistemini oluşturan dedektör ve elektronik cihazların şematik ve gerçek görüntüleri)

All concretes were measured using the same reference measurement. After that, the samples were positioned between the detector and the source. Concrete radiation absorption coefficients were determined using ¹³⁷Cs and ⁶⁰Co radioactive

sources in tests conducted at 662 keV, 1173 keV, and 1332 keV energies. In the experiments, it will be ensured that the sample is at an equal distance between the source and the detector, as shown in Figure 4.

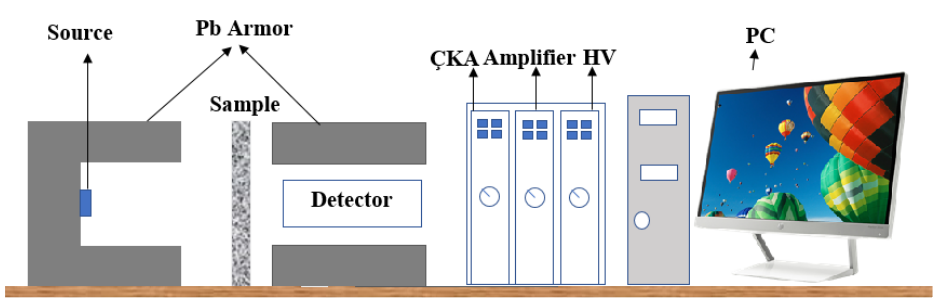


Figure 4. Detector and electronic devices that make up the gamma spectroscopy system (Gama spektroskopisi sistemini oluşturan dedektör ve elektronik cihazlar)

The linear attenuation coefficient (μ) is the probability of radiation interaction with a material per unit path length. The mass attenuation coefficient (μ/ρ) is the probability of all types of interactions (photoelectric, Compton, and pair production) per unit mass density. Parameters such as effective atomic number, effective electron density, half-value layer (HVL), mean free path (MFP), and X-ray and gamma-ray transmission factors can be calculated using the mass attenuation coefficient [24].

$$\frac{\mu}{\rho} = \left(-\frac{1}{\rho x}\right) \ln\left(\frac{I}{I_0}\right) \tag{3}$$

Where x is the thickness of the absorbing material, I_0 and I represent the initial radiation intensity and transmission, respectively.

The total mass attenuation coefficient (μ_{total}) is the aggregate of the attenuation coefficients for

photoelectric absorption, Compton scattering, and pair production for a particular energy photon [25].

$$\mu_{total} = \mu_{photoelectric} + \mu_{compton} + \mu_{pair-production}$$
 (4)

Half-value layer (HVL) is the thickness of radiation shielding required to reduce the radiation intensity by half compared to the initial radiation intensity. Meanwhile, Tenth-value layer (TVL) is the thickness of radiation shielding required to reduce the radiation intensity by one-tenth compared to the initial radiation intensity. Both parameters can be calculated using the equation [26]:

$$HVL = \ln 2/\mu \tag{5}$$

$$TVL = \ln 10/\mu \tag{6}$$

Mean free path (MFP) is a concept used to measure the average distance traveled by particles or photons in a medium before they interact or collide with other particles. Low-energy photons lose their energy over shorter distances, while high-energy photons require longer distances. This parameter is defined as a statistical measure used to describe how often particles or photons will interact in a specific medium. MFP can be calculated using the value of the linear attenuation coefficient [27]:

$$\lambda = \frac{1}{\mu} \tag{7}$$

WinXCOM was established to calculate photon interaction cross-sections and mass attenuation coefficients for different combinations of elements, compounds, or mixtures across energy levels ranging from 1 keV to 100 GeV. This popular and widely used tool was recently converted to the Windows platform. Many people have now modified this standalone program to run in the Windows environment. For an energy grid set at

standard values with points roughly logarithmically separated, or for a user-specified grid, WinXCom can produce cross-sections or attenuation coefficients. In addition to providing complete mass attenuation coefficients for compounds, it also presents partial cross-sections for pair production, coherent scattering, incoherent scattering, and photoelectric absorption. Additionally, as total attenuation coefficients are frequently employed in gamma-ray transport calculations, they provide these without the contribution of coherent scattering.

2. **RESULTS** (BULGULAR)

In this study, experiments were carried out on 3 samples from each series. The density values of the produced samples are given in Figure 5.

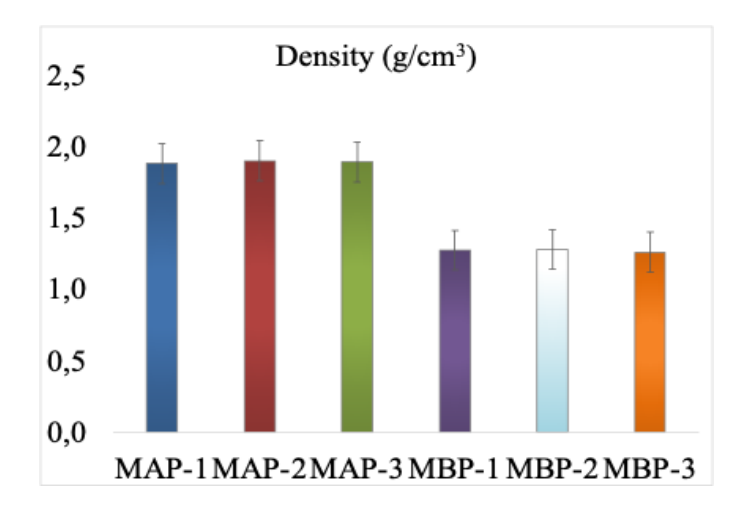


Figure 5. Density values of samples (Numunelerin yoğunluk değerleri)

Kilincarslan et al. (2018) [14] produced foam concrete with Portland cement using Isparta-Karakaya pumice. They obtained the 28-day compressive strength values of the foam concretes with a density of 0.551 g/cm³ as 8 MPa and the thermal conductivity values as 0.14 W/ mK.

Concrete radiation shielding coefficients were determined using ¹³⁷Cs and ⁶⁰Co radioactive sources in tests conducted at 662 keV, 1173 keV, and 1332 keV energies. The radiation retention coefficient values of the samples are given in Figure 6.

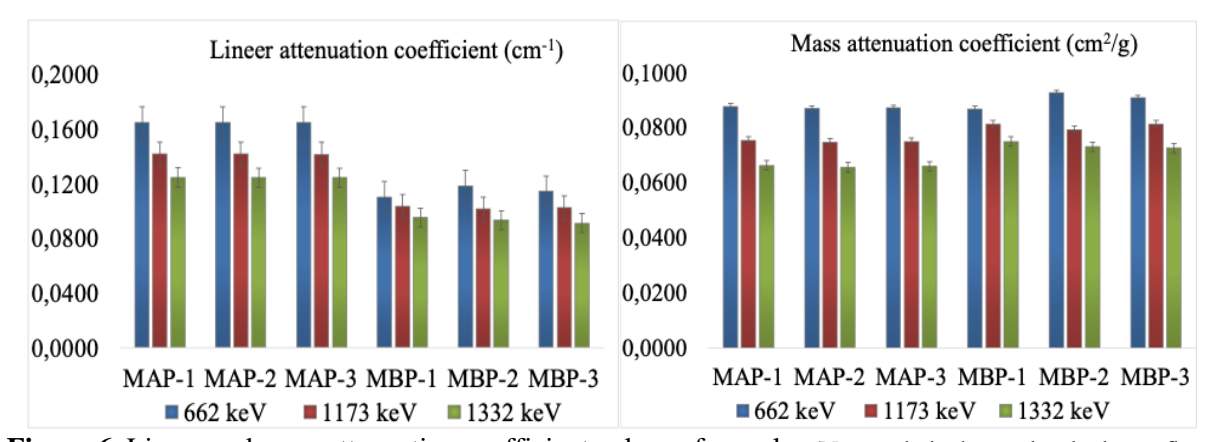


Figure 6. Lineer and mass attenuation coefficient values of samples (Numunelerin doğrusal ve kütle zayıflama katsayısı değerleri)

The findings in the table compare the linear and mass attenuation coefficients of MAP and MBP materials at different energies (662 keV, 1173 keV, and 1332 keV) and reveal the radiation attenuation performances of these materials. In terms of linear attenuation coefficient, it is observed that MAP has higher values compared to MBP at all energies. MAP, which shows a higher linear attenuation coefficient of 44% at 662 keV, 38% at 1173 keV, and 33% at 1332 keV, contributes to the absorption of photons. However, this difference decreases as the energy increases, i.e., the superiority of MAP for high-energy photons decreases relatively. The main reason for this is that the probability of high-energy photons interacting with the material decreases, and they can penetrate deeper. On the other hand, when evaluated in terms of mass attenuation coefficient, it is observed that MBP has higher values compared to MAP. With a higher mass attenuation coefficient of 3% at 662 keV, 7.5% at 1173 keV, and 11.5% at 1332 keV, MBP shows more radiation attenuation per unit mass. This indicates that MBP is advantageous in terms of low density while maintaining a relatively strong attenuation capacity. The fact that the mass attenuation advantage of MBP increases as the energy increases indicates that this material can be an effective option for highenergy photons.

In many different applications, radiation concrete is essential for preventing damaging ionizing radiation [28,29]. It is an essential component of reactor containment buildings, spent fuel storage, and waste disposal facilities in nuclear power plants, and it is vital for protecting both the environment and employees. To provide a secure environment for patients, employees, and guests, medical facilities also use radiation shielding concrete to construct the walls, floors, and ceilings of diagnostic imaging and radiation therapy rooms [30]. Additionally, it is necessary for industrial radiography facilities, which allow for safe non-destructive testing in the construction, automotive, and aerospace industries [31, 32]. Radiation shielding concrete is essential to the safety and compliance of research labs that work with radioactive materials. It is used by the military in command centers and bunkers to shield equipment and people from nuclear threats. By isolating radioactive materials in nuclear waste storage, radiation shielding concrete stops radiation from seeping into the surrounding environment [33]. Additionally, it protects employees when handling and producing medicinal isotopes in radiopharmaceutical manufacturing. All things considered, radiation-shielding concrete is essential for maintaining safety and legal compliance while promoting the advantageous application of radiation in various industries. HVL and TVL values of the sample are given in Figure 7, and MFP values are given in Figure 8. In Figures 7 and 8, the first three bars show MAP values and the last three bars show MBP values.

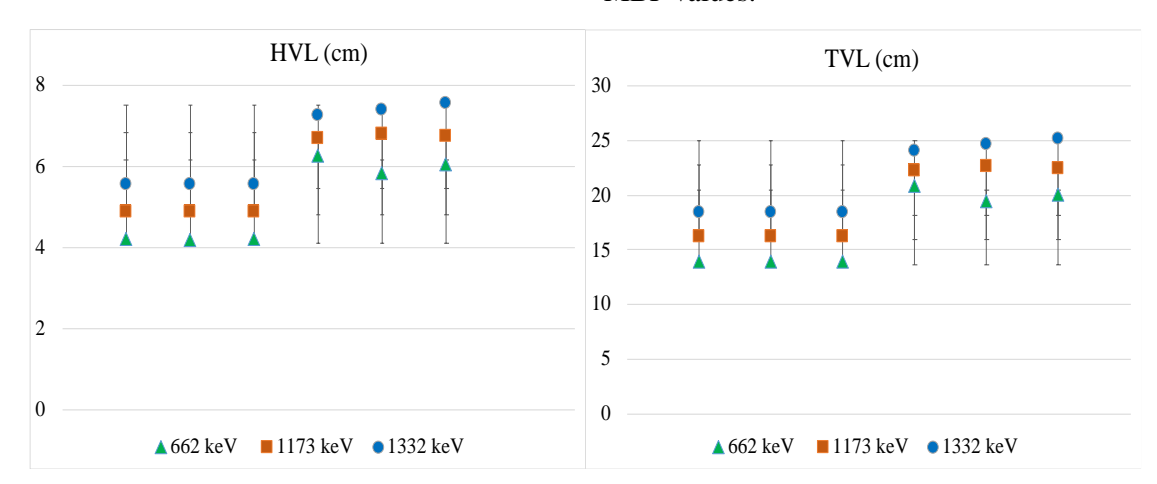


Figure 7. HVL and TVL values of the samples at 662 keV, 1173 keV and 1332 keV energies (662 keV, 1173 keV ve 1332 keV energielerindeki numunelerin HVL ve TVL değerleri)

When the HVL and TVL values are evaluated, it is seen that both the HVL and TVL values of the MBP material are higher than those of MAP at all energies. For example, at 662 keV, the HVL for MAP is 4.20 cm, while it is 6.05 cm for MBP, meaning that the half-value thickness of MBP is 44% higher than that of MAP. Similarly, at 1332 keV, the HVL for MAP is 5.56 cm, while it is 7.42

cm for MBP, indicating that MBP requires more thickness. A similar trend is observed in terms of TVL values; at 662 keV, the TVL value of MAP is 13.95 cm, while it is 20.12 cm for MBP, indicating that MBP requires 44% more thickness than MAP to reduce the radiation to one-tenth.

These results show that MAP is a better attenuator compared to MBP, that is, it absorbs more radiation with less material. The difference is more pronounced, especially at low energies, and it is seen that the difference decreases as the energy increases. While the difference between MAP and MBP decreases at 1332 keV, it is still understood

that MAP is a better attenuator. These findings show that MAP is a more advantageous material for effective protection with a thinner layer in radiation shielding applications, but MBP can also be considered if other factors, such as lightness or cost, come into play. The MFP values obtained in the study are given in Figure 8.

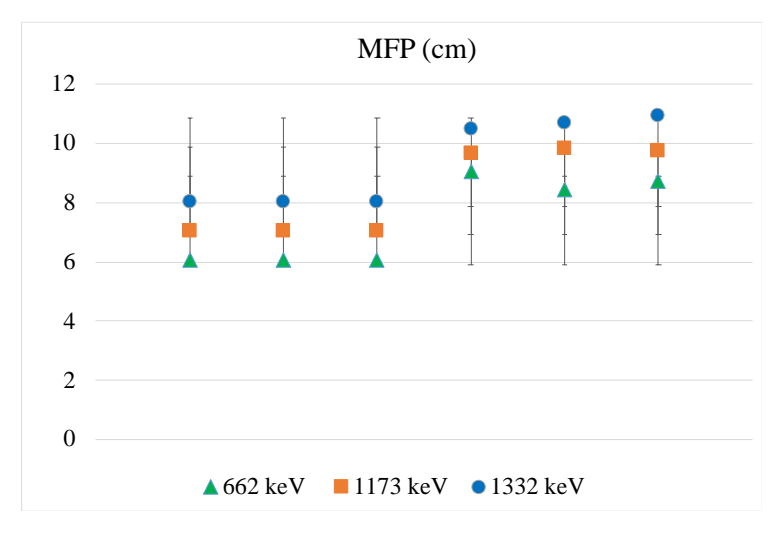


Figure 8. MFP values of the samples at 662 keV, 1173 keV and 1332 keV energies (662 keV, 1173 keV ve 1332 keV energierindeki numunelerin MFP değerleri)

Mean free path values at 662 keV energy are on average 6.059037 in MAP samples and 7.661328 in MBP samples. Mean free path values at 1173 keV energy are on average 7.050643 in MAP samples and 8.885692 in MBP samples. Mean free path values at 1332 keV energy are on average 8.021529 in MAP samples and 10.703606 in MBP samples. The difference between MAP and MBP samples is also clearly seen in the Mean Free Path (MFP) values. MFP shows how far photons can travel in a material without colliding and expresses the permeability of the material to the photon beam. At 662 keV, 1173 keV, and 1332 keV, the MFP values of the MAP sample are lower than those of the MBP sample at each energy level. For example, at 662 keV, the MFP value of the MAP sample is 6.059037, while that of the MBP sample is 7.661328. This indicates that the MAP sample causes photons to collide at shorter distances; therefore, the photons are absorbed more quickly in the material. It is observed that MFP values increase as energy increases in both samples. This is related to the fact that as photon energy increases, photons are attenuated less in the material and can travel

longer distances. In general, the MBP sample allows photons to travel longer distances than the MAP sample because the MFP values of the MBP are higher at each energy level. This means that the MBP has a lower attenuation of the photon beam, and the photons are free to move in this material for a longer time. The MAP sample, on the other hand, has shorter MFP values, which means that the photons attenuate more quickly and collide at shorter distances.

The values obtained at 662 keV, 1173 keV, and 1332 keV energies, because of entering the data into the WinxCOM program output examples are given in Figure 9 for the MAP sample and Figure 10 for the MBP sample.

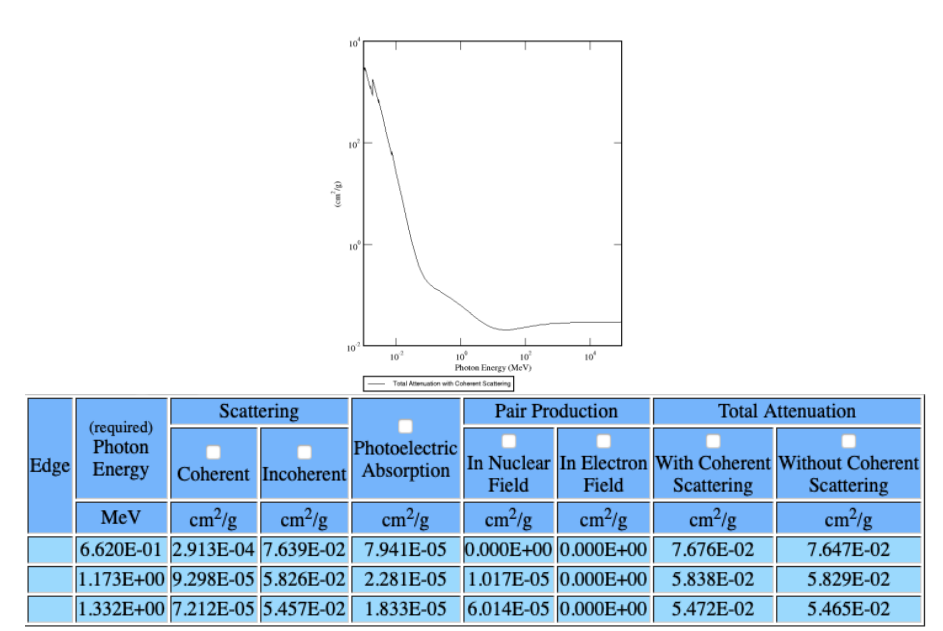


Figure 9. WinxCOM mass attenuation coefficient values of the MAP sample at 662 keV, 1173 keV and 1332 keV energies (MAP örneğinin 662 keV, 1173 keV ve 1332 keV enerjilerindeki WinxCOM kütle zayıflama katsayısı değerleri)

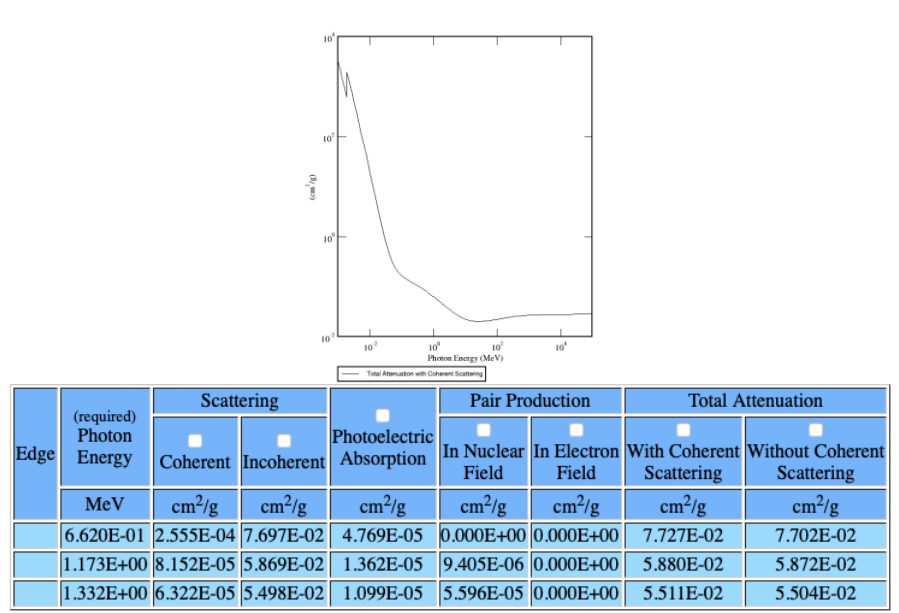


Figure 10. WinxCOM mass attenuation coefficient values of the MBP sample at 662 keV, 1173 keV and 1332 keV energies (MBP örneğinin 662 keV, 1173 keV ve 1332 keV enerjilerindeki WinxCOM kütle zayıflama katsayısı değerleri)

The mass attenuation coefficient values of the MAP samples obtained according to the experimental and XCOM analysis results are given in Figure 11, and

the mass attenuation coefficient values of the MBP samples are shown in Figure 12.

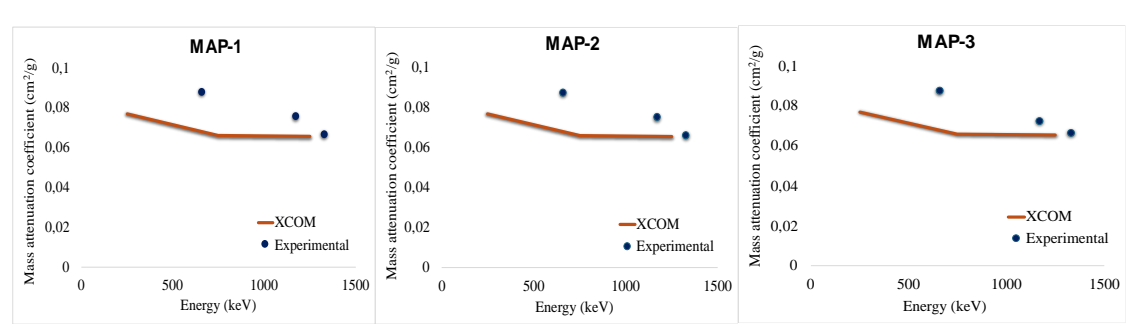


Figure 11. Experimental and XCOM values of the MAP sample (MAP örneğinin deneysel ve XCOM değerleri)

Figure 12. Experimental and XCOM values of the MBP sample (MBP örneğinin deneysel ve XCOM değerleri)

It is observed that the experimental results are slightly higher than the XCOM values at all energy levels (662 keV, 1173 keV, and 1332 keV). For example, for MAP 1, the experimental value at 662 keV is 0.0878 while the XCOM value is 0.07676, which is approximately 14.4% higher than the experimental measurement. Similarly, at 1173 keV, the experimental value is 0.0754 while the XCOM is 0.0659, which is also approximately 14.4% higher. At 1332 keV, the difference decreases to 1.2%. Similar trends are also valid for MAP 2 and MAP 3. The experimental value of MAP 2 at 662 keV is 0.0869, which is 13.2% higher than XCOM, but this difference decreases to 0.5% at 1332 keV. The same trend continues for MAP 3, there is a difference of 13.6% at 662 keV, decreasing to 0.5% at 1332 keV. These findings show that the experimental results are higher than the XCOM calculations at low energies, but the difference decreases as the energy increases. In general, it was determined that there is a good agreement between the XCOM data and the experimental findings.

The results of this study suggest that both MAP and MBP concretes possess unique properties that make them suitable for specific industrial applications. MAP concretes, which demonstrate high radiation shielding capacity, are particularly promising for use in nuclear facilities, medical radiology rooms, and research laboratories where exposure to gamma and X-ray radiation is a critical concern. Their ability to attenuate radiation efficiently, combined with satisfactory mechanical performance, ensures both safety and structural integrity in such environments. On the other hand, MBP concretes, incorporating lightweight aggregates such as pumice, offer reduced density while maintaining adequate mechanical properties. These characteristics make MBP concretes ideal for where weight applications reduction advantageous, such as in high-rise buildings, longspan structures, or modular construction. The reduced dead load can lead to lower structural demands, cost savings, and improved seismic performance, all while maintaining environmental

benefits due to the use of sustainable aggregates. Overall, the selection between MAP and MBP concretes should consider both functional requirements such as radiation shielding versus lightweight structural performance and environmental and economic factors. These insights highlight the versatility of MOC-based concretes and point to opportunities for further optimization in industrial applications.

3. CONCLUSIONS (SONUÇLAR)

In conclusion, the findings of this study provide a comprehensive comparison of the radiation attenuation properties of MAP and MBP materials at different photon energies, highlighting their respective advantages in radiation shielding applications. The linear attenuation coefficient analysis demonstrates that MAP exhibits superior photon absorption capabilities compared to MBP across all energy levels, with the difference being more pronounced at lower energies. This indicates that MAP is a more effective shielding material for lower-energy photons, where the probability of interaction is higher. However, as photon energy increases, the difference between MAP and MBP decreases, suggesting that high-energy photons penetrate both materials more easily, reducing MAPs relative advantage. In contrast, the mass attenuation coefficient results reveal that MBP performs better than MAP in terms of radiation attenuation per unit mass, particularly at higher energies. This suggests that MBP could be a more efficient choice when material density or weight reduction is a key consideration, making it potentially advantageous in applications where lightweight shielding is required.

The HVL and TVL values further reinforce these observations by showing that MBP requires greater thickness than MAP to achieve the same level of radiation attenuation. At all photon energies, both HVL and TVL values for MBP are higher than those of MAP, emphasizing that MAP is a more effective attenuator, requiring less material to achieve the

desired shielding effect. This property makes MAP a preferable option in scenarios where space and material efficiency are critical. However, the increasing HVL and TVL differences at higher energies also indicate that MBP's relative effectiveness improves as energy increases. The MFP results also align with these trends, as MAP consistently exhibits lower MFP values than MBP, confirming that photons travel shorter distances before undergoing interactions in MAP. This indicates that MAP can attenuate photons over a shorter distance, further confirming its effectiveness as a shielding material. On the other hand, MBP 's higher MFP values indicate that it allows photons to travel longer distances without interactions, making it less effective for shielding but potentially suitable for other applications where controlled photon transmission is required.

Additionally, the comparison between experimental and XCOM data reveals a consistent trend where experimental attenuation values are slightly higher than XCOM predictions, particularly at lower energies. Despite these differences, the overall agreement between experimental and XCOM data suggests that theoretical models provide reliable estimates for attenuation coefficients, with experimental validation offering valuable refinements. Overall, these findings highlight that acidic pumice is a highly effective material for radiation shielding, especially in applications requiring compact, high-performance barriers. However, basic pumice remains a viable alternative in applications where material density and weight considerations play a crucial role. The study highlights the importance of selecting shielding materials based on specific application needs, energy levels, and practical constraints, ensuring optimal radiation protection in various scenarios.

DECLARATION OF ETHICAL STANDARDS (ETİK STANDARTLARIN BEYANI)

The author of this article declares that the materials and methods they use in their work do not require ethical committee approval and/or legal-specific permission.

Bu makalenin yazarı çalışmalarında kullandıkları materyal ve yöntemlerin etik kurul izni ve/veya yasal-özel bir izin gerektirmediğini beyan ederler.

AUTHORS' CONTRIBUTIONS (YAZARLARIN KATKILARI)

Semsettin KILINÇARSLAN: He conducted the experiments, analyzed the results and performed the writing process.

Deneyleri yapmış, sonuçlarını analiz etmiş ve maklenin yazım işlemini gerçekleştirmiştir.

Yasemin ŞİMŞEK TÜRKER: He conducted the experiments, analyzed the results and performed the writing process.

Deneyleri yapmış, sonuçlarını analiz etmiş ve maklenin yazım işlemini gerçekleştirmiştir.

Nuri IŞILDAR: He conducted the experiments, analyzed the results and performed the writing process.

Deneyleri yapmış, sonuçlarını analiz etmiş ve maklenin yazım işlemini gerçekleştirmiştir.

CONFLICT OF INTEREST (ÇIKAR ÇATIŞMASI)

There is no conflict of interest in this study.

Bu çalışmada herhangi bir çıkar çatışması yoktur.

REFERENCES (KAYNAKLAR)

- [1] Jankovský O, Lojka M, Lauermannová AM, Antonc ík F, Pavlíková M, Pavlík Z, Sedmidubský D, Carbon dioxide uptake by MOC-based materials, Appl. Sci. 2020; 10: 2254.
- [2] Chen X, Zhang T, Bi W, Cheeseman C. Effect of tartaric acid and phosphoric acid on the water resistance of magnesium oxychloride (MOC) cement, Constr. Build. Mater. 2019; 213: 528-536
- [3] Jin YJ, Xiao LG, Luo F. Influence of calcium added slag on the strength and water-repellency of magnesium oxychloride cement, Appl. Mech. Mater. 2013; 278-280: 437-439.
- [4] Huang Q, Zheng W, Xiao X, Dong J, Wen J, Chang C. Effects of fly ash, phosphoric acid, and nano-silica on the properties of magnesium oxychloride cement. Ceramics International. 2021; 47: 34341–34351.
- [5] Guo Y, Zhang Y, Soe K, Pulham M. Recent development in magnesium oxychloride cement. Structural Concrete. 2018; 19(5): 1290–1300.
- [6] He P, Poon CS, Tsang DC. Using incinerated sewage sludge ash to improve the water resistance of magnesium oxychloride cement (MOC). Construction and Building Materials. 2017; 147: 519–524.
- [7] Madani H, Norouzifar MN, Rostami J. The synergistic effect of pumice and silica fume on the durability and mechanical characteristics of eco-friendly concrete. Construction and Building Materials. 2018; 174: 356–368.
- [8] Szabó R, Kristaly F, Nagy S, Singla R, Mucsi G, Kumar S. Reaction, structure and properties of

- eco-friendly geopolymer cement derived from mechanically activated pumice. Ceramics International. 2023; 49(4): 6756–6763.
- [9] Deniz V, Umucu Y, Yılmaz İ. Evaluation of Jig Performances in Pumice Enrichment Plant of Industrial Minerals Inc. In: Akar A, Seyrankaya A, editors. 5th Industrial Raw Materials Symposium; 2004; Izmir, Turkey. p. 307–312.
- [10] Binici H, Durgun MY, Rizaoğlu T, Koluçolak M. Investigation of durability properties of concrete pipes incorporating blast furnace slag and ground basaltic pumice as fine aggregates. Scientia Iranica. 2012; 19(3): 366–372.
- [11] Tapan M, Depci T, Özvan A, Efe T, Oyan V. Effect of physical, chemical and electro-kinetic properties of pumice on strength development of pumice blended cements. Materials and Structures. 2013; 46: 1695–1706.
- [12] Hossain KMA, Properties of volcanic pumice-based cement and lightweight concrete. Cement and Concrete Research, 2004; 34: 2, 283-291.
- [13] Kilincarslan Ş, Davraz M, Akça M. The effect of pumice as aggregate on the mechanical and thermal properties of foam concrete, Arab. J. Geosci. 2018; 11: 1-6.
- [14] Kilinçarslan Ş, Davraz M, Akça M. Investigation of the properties of pumice aggregate foam concretes, J. Eng. Sci. 2018; 6 (1): 148-153.
- [15] Ersoy B, Sariisik A, Dikmen S, Sariisik G. Characterization of acidic pumice and determination of its electrokinetic properties in water, Powder Technol. 2010; 197 (1-2): 129-135.
- [16] Yücel HE, Öz HÖ, Güneş M. The effects of acidic and basic pumice on physicomechanical and durability properties of self-compacting concretes, Green Build. Constr. Econ. 2020; 21-36.
- [17] Öz HÖ. Properties of pervious concretes partially incorporating acidic pumice as coarse aggregate, Constr. Build. Mater. 2018; 166: 601-609.
- [18] Soleimani A, Mahvi AH, Yaghmaeian K, Abbasnia A, Sharafi K, Alimohammadi M, Zamanzadeh M. Effect of modification by five different acids on pumice stone as natural and low-cost adsorbent for removal of humic acid from aqueous solutions-Application of response surface methodology. J Mol Liq. 2019; 290: 111181.
- [19] Çifçi Dİ, Meriç S. A review on pumice for water and wastewater treatment. Desal Water Treat. 2016; 57(39): 18131–18143.
- [20] Tanyıldızı M, Gökalp İ. Utilization of pumice as aggregate in the concrete: A state of art. Constr Build Mater. 2023; 377: 131102.

- [21] Gündüz L, Sarıışık A, Tozaçan B, Davraz M, Uğur İ, Çankıran O. Pumice Technology (Pumice Characterization). Isparta; 1998. p. 285.
- [22] Akkurt I, Akyıldırım H, Mavi B, Kilincarslan S, Basyigit C. Photon attenuation coefficients of concrete includes barite in different rate. Ann Nucl Energy. 2010a; 37(7): 910–914.
- [23] Akkurt I, Akyıldırım H, Mavi B, Kilincarslan S, Basyigit C. Radiation shielding of concrete containing zeolite. Radiat Meas. 2010b; 45(7): 827–830.
- [24] Tellili B, Elmahroug Y, Souga C. Investigation on radiation shielding parameters of cerrobend alloys. Nucl Eng Technol. 2017; 49(8): 1758–1771.
- [25] Alsaab AH, Zeghib S. Analysis of X-ray and gamma ray shielding performance of prepared polymer micro-composites. J Radiat Res Appl Sci. 2023; 16(4): 100708.
- [26] Gunoglu K, Akkurt I. Radiation shielding properties of concrete containing magnetite. Prog Nucl Energy. 2021; 137: 103776.
- [27] Matori KA, Sayyed MI, Sidek HAA, Zaid MHM, Singh VP. Comprehensive study on physical, elastic and shielding properties of lead zinc phosphate glasses. J Non-Cryst Solids. 2017; 457: 97–103.
- [28] Ban CC, Khalaf MA, Ramli M, Ahmed NMA, Ahmad MS, Ali AMA, et al. Modern heavyweight concrete shielding: principles, industrial applications and future challenges; review. J Build Eng. 2021; 39: 102290.
- [29] Kanagaraj B, Anand N, Andrushia AD, Naser MZ. Recent developments of radiation shielding concrete in nuclear and radioactive waste storage facilities a state-of-the-art review. Constr Build Mater. 2023; 404: 133260.
- [30] Al-Buriahi MS, Alzahrani JS, Alrowaili ZA, Olarinoye IO, Sriwunkum C. Recycling of waste cathode-ray tube glasses as building materials for shielding structures in medical and nuclear facilities. Constr Build Mater. 2023; 376: 131029.
- [31] Zayed M, El Khayatt AM, Petrounias P, Shahien MG, Mahmoud KA, Rashad AM, et al. From discarded waste to valuable products: barite combination with chrysotile mine waste to produce radiation-shielding concrete. Constr Build Mater. 2024; 417: 135334.
- [32] Zhang P, Wittmann FH, Zhao T, Lehmann EH, Vontobel P. Neutron radiography, a powerful method to determine time-dependent moisture distributions in concrete. Nucl Eng Des. 2011; 241: 4758–4766.

[33] Wisnubroto DS, Zamroni H, Sumarbagiono R, Nurliati G. Challenges of implementing the policy and strategy for management of radioactive waste and nuclear spent fuel in Indonesia. Nucl Eng Technol. 2021; 53: 549–561